Some Problems Associated with Wind Drag and Infrared Images of the Sea Surface[1]

JAMES R. MCGRATH AND M. F. M. OSBORNE

Naval Research Laboratory, Washington, D. C. 20375

(Manuscript received 11 September 1972, in revised form 26 March 1973)

ABSTRACT

It is argued that there should be a close connection between fluctuations in infrared images of the sea and fluctuations in wind drag on the sea. The critical regions of wind speed, temperature, and surface contaminant, where these fluctuations should be largest, are pointed out. Some examples are given of infrared ocean images and the problems associated with their interpretation.

1. Introduction

In two previous papers, Osborne (1964, 1965) showed that fluctuations of less than 1C in infrared (IR) images of the ocean surface could be accounted for, in part, by variations in the laminar, air and water boundary-layer thicknesses, δ_a and δ_w, respectively, at the air-sea interface. Since that time there has been an increasing commercial availability of infrared mapping devices (Stingelin, 1969; Kelton *et al.*, 1963; Ballard, 1959) and greater understanding of some of the complexities of thermal phenomena at the air-sea interface as discussed by Clark (1967), Hill (1972), Hasse (1971) and McGrath (1971). This paper briefly summarizes some of the problems of oceanic IR image interpretation and illustrates them with examples of real data hitherto publicly not available. These are taken from aircraft at altitudes $\leqslant 1000$ m, primarily, but not exclusively, at night.

Using Osborne's model of the ocean surface, the energy balance equation which is used to determine the radiation temperature T_0 of the ocean surface is

$$\sigma(T_s^4-T_0^4)+[k_a(T_a-T_0)/\delta_a]+[k_w(T_w-T_0)/\delta_w]+[\omega_D L(\rho_{amb}-\rho_{sat})/\delta_a]=0, \quad (1)$$

where the heat flux terms can be identified as being due to radiation, air conduction, water conduction and evaporation, respectively. Note that this is a steady-state formula, which implies that the time constants τ_a and τ_w for cooling the air and water layers, respectively, must be smaller than characteristic time intervals over which natural thermal processes occur, say, the bulk water or air changes its temperature by an amount $\sim$1C. This, in turn, means that the thicknesses must be small, less than 1–2 mm, which they usually are at night. Visible radiation tends to make the water convectively stable, implying a much thicker unstirred laminar surface layer and correspondingly larger water time constant during the day.

Eq. (1) is solved for T_0, which is expressed as corrections to the underlying bulk water temperature, T_w, i.e.,

$$T_0=T_w+(T_a-T_w)(k_a\delta_w/k_w\delta_a)+(T_s-T_w)(4\sigma T_w^3\delta_w/k_w)+\omega_D L\delta_w(\rho_{amb}-\rho_{sat})/(k_w\delta_a), \quad (2)$$

or

$$T_0=T_w+\Delta T_c+\Delta T_r+\Delta T_e,$$

where the correction terms ΔT_c, ΔT_r and ΔT_e are of the order 1C. The first term ΔT_c represents collectively air and water conduction and is usually numerically smaller than the radiation term ΔT_r or evaporation term ΔT_e.

The variation in position and time of the correction terms provides most of the difficulties in interpreting IR images. Variations in T_w obviously enter directly, but the experimenter is frequently confronted with an image which is presumably a homogeneous ocean surface which shows many patterns (or structure) in one part of the picture and a different pattern (or none) elsewhere. Two images taken under similar situations often show great differences in thermal detail. The question is, why?

Examination of numerical values from (2) shows that δ_a and δ_w are the principal sources of variation in the correction terms. These can easily vary by a factor of 2 from one instant, or position on the sea, to a neighboring instant or position. These variations correspond to changes in T_0 of $\sim$0.5C. The sky temperature T_s is the next most significant source of variation at night: from clear, $T_s\approx 243$K, to overcast, $T_s\approx 273$K, with $T_w\approx 293$K. Still larger changes in T_s

[1] Taken in part from a dissertation submitted by one of the authors (JRM) to the Faculty of the Graduate School of The Catholic University of America, Washington, D. C., in partial fulfillment of the requirements for the Doctor of Philosophy degree.

occur during the day, owing to the presence or absence of direct sunlight.

In the absence of an appreciable radiation term, $\Delta T_r \approx 0$ (that is, when $T_s \approx T_w$), only the variation of the ratio δ_w/δ_a enters into the "signal" $T_0 - T_w$. Most laboratory tank experiments are conducted with the "sky" at room temperature; hence, such experiments cannot directly disentangle (using IR alone) the separate variations of δ_a and δ_w.

We now want to identify, briefly, the conditions under which δ_a and δ_w are likely to change most rapidly. The IR image is interpreted as a picture of thermal energy flux from the ocean. There is also a momentum flux which is similarly determined in large part by similar or proportional δ's:

$$\delta_{a,\text{thermal}} = C_a \delta_{a,\text{mom}}, \quad \delta_{w,\text{thermal}} = C_w \delta_{w,\text{mom}}.$$

The constants of proportionality, C_a and C_w, depend on the Prandtl number. So if we can identify the conditions under which δ_a and δ_w for momentum change most rapidly, we can also (presumably) identify the conditions under which the IR image shows the most variation or structure.

2. Variations in boundary-layer thickness

The boundary-layer thicknesses, δ_a and δ_w, change most rapidly when there are large fluctuations in the drag coefficient of the wind on the sea or changes from one form of dynamical stability to another. Experimentally, according to Ruggles (1970), the biggest fluctuations in drag occur at wind speeds of $U_{10} = 2$, 4, 8 m sec^{-1}. There is another shift at $U_{10} = 15$ m sec^{-1}, which according to Wu (1971a), is due to the onset of spray generation. These are the wind speeds at which we expect the greatest change in the "complexion" of an IR image. We do not know whether this is, in fact, the case, but a relation between fluctuations in drag and fluctuations in IR images should exist because both are related to momentum transfer through the boundary layer thicknesses.

Lock (1951) and Osborne (1964) have pointed out a different type of singular behavior in δ_a and δ_w when either the air or water velocities approach zero. In fact, it was this theoretical phenomenon which first attracted our attention to the possibility of abrupt changes in δ_a and δ_w. The experience here at the Naval Research Laboratory has been that IR images under conditions of near calm ($U_{10} \approx 0$) are the most difficult and complicated types to interpret. Thus, there are five different air velocities in all (0, 2, 4, 8, 15 m sec^{-1}) in the neighborhood of which we expect pronounced boundary layer thickness changes.

A second type of dynamical stability-instability transition is suggested by Eq. (2) itself. If $T_0 > T_a$ the air is heated by conduction from below and is convectively unstable. This results in a thin and relatively well-defined air laminar boundary layer. If $T_0 < T_w$ the water is cooled from above, it is convectively unstable, and we have a well-defined water boundary layer. The thicknesses can be estimated from the criterion for Rayleigh instability under the condition of a constant heat flux, i.e., constant temperature gradient (Landau and Lifschitz, 1959) and are of the order of 1 mm.

So from Eq. (2) we have as conditions in the neighborhood of which the boundary layers change rapidly in effective thickness:

$$T_a - T_0 = 0,$$

or

$$-(T_w - T_a + \Delta T_c + \Delta T_r + \Delta T_e) = 0 \begin{cases} \text{air instability}, & T_a - T_0 < 0 \\ \text{air stability}, & T_a - T_0 > 0 \end{cases} \tag{3}$$

$$T_0 - T_w = 0,$$

or

$$\Delta T_c + \Delta T_r + \Delta T_e = 0 \begin{cases} \text{water instability}, & T_0 - T_w < 0 \\ \text{water stability}, & T_0 - T_w > 0 \end{cases} \tag{4}$$

Eq. (3) implies a relation between thermal structure and drag which is, in fact, observed. Cold air over a warm sea gives thinner boundary layers (hence more drag) than the converse (Roll, 1965). The radiation term ΔT_r indicates that there may be two aspects of this phenomenon, which to the best of our knowledge have not been distinguished. If on a clear day with a good wind, the sun is abruptly obscured by a cloud, the sea may become rougher. This is not the same as an abrupt shift from a hot wind to a cold wind, although the air may feel cooler. The sky (sun) temperature has changed abruptly, so that the sea surface which was previously warmed by net radiation (ΔT_r) plus evaporation (ΔT_e) is now being net cooled. The result is an instability and a thinner boundary layer (more drag) on the water. A change in humidity (ambient water vapor density ρ) could have a similar effect.

Note that the three correction terms appear with opposite signs in the two stability criteria [Eqs. (3) and (4)]. Thus a stability-instability shift in the water [(4)], say, due to radiation changes, may be accompanied by a shift in the opposite sense in the air [(3)]. Such a coupling might account for the bi-modal behavior of the drag coefficient observed by Ruggles (1970).

As a third possibility, δ_a and δ_w may change abruptly due to changes in the boundary conditions themselves—continuity of the normal and tangential velocity [for a contrary view, see Schmitz (1962)] and prescribed discontinuities in the normal p_n and tangential stress p_t (Batchelor, 1967; Osborne, 1968). The stress dis-

continuities may be written

$$p_{n_1}-p_{n_2}=\pi(R_1^{-1}+R_2^{-1})|_{z=\zeta}, \quad (5)$$

and

$$p_{tx1}-p_{tx2}=\frac{\partial}{\partial y}\left[\mu_s\left(\frac{\partial u}{\partial y}+\frac{\partial u}{\partial x}\right)+\frac{\partial \pi}{\partial x}\right]\Bigg|_{z=\zeta}, \quad (6)$$

for the x-component of p_t; a similar expression holds for the y-component. Here R_1 and R_2 are the principal radii of curvature of the interface $z=\zeta(x,y,t)$; and π and μ_s are the surface tension and surface viscosity, respectively. These are constant for a clean surface; with a surface contaminant they depend on the surface concentration which, in turn, is affected by the surface convergence of the underlying flow and rates of absorption and desorption. The surface stress discontinuities in (5) and (6) are only for the simplest case, where the film can be described by only two rheological coefficients, π and μ_s. Goodrich (1962) considers more complicated films. Note that the tangential stress discontinuities are largely associated with horizontal *variations* in the surface parameters, μ_s and π.

Considerable theory and experiment exist on the effect of these stress discontinuities on wave generation (Garrett, 1967; Goodrich, 1962) but not much is known from theory about their effect on boundary layer thickness. That they do have an effect is well known experimentally, however. The most obvious evidence is that they thicken the laminar boundary layer and hence reduce the drag. A slick is calmer than clean water in the presence of wind. This is consistent with the observation that slicks are radiometrically cooler than adjacent ocean surfaces.

We regard the complications added by surface contaminants as usual, rather than exceptional, aspects of air-sea interaction. Natural bodies of water usually have small amounts of surface contaminants (McDowell and McCutcheon, 1971). The work of Garrett (1967) shows very clearly that at quite low values of surface contaminant concentration, the effect on capillary wave damping rises steeply to a maximum, and it is the behavior of capillary waves which determines in large measure the surface roughness, horizontal momentum transport and hence (presumably) the effective laminar boundary layer thickness.

We must mention an implied assumption in the argument relating drag changes, temperature changes, and boundary layer thickness changes, which is subject both to misinterpretation and dispute. The implied assumption (Wu, 1971b) is that the horizontal stress in the turbulent air, ρu^{*2} (u^* being determined from the mean velocity profile with height), is predominantly transmitted to the water via the horizontal component of tangential stress, i.e., $\overline{p_t \cos\alpha}$, where α is the angle of slope of the interface $z=\zeta(x,y,t)$ and the bar indicates a time and space average. This assumption is equivalent to assuming the profile drag on the surface (the horizontal component of normal stress), $\overline{p_n \sin\alpha}$, is relatively small for the purpose of transferring horizontal momentum. For the purpose of wave generation, we are not making any assumptions about the relative importance of normal and tangential stress. This is a different question which is also subject to dispute.

Arguments in favor of our implied assumption are given by Phillips (1966). Evidence to the contrary, i.e., that $\overline{p_n \sin\alpha}$ is the dominant source of horizontal momentum transport, is given by Dobson (1971). We do not know what the resolution of either of these controversies is.

3. The effects of emissivity, air transmission and convergence

Finally, there are sources of apparent variations in T_0 which we have not yet discussed, sources involving variations in surface emissivity, air transmission, and convergence in flow. Clark (1967) and Boudreau (1965) have discussed the first two of these effects. Some numbers from the latter reference will illustrate the order of magnitude of their importance.

If the transmissivity of the air is 0.75 ± 0.02 and the emissivity of the sea is 0.96 ± 0.01, the apparent fluctuation in T_0 corresponding to the indicated standard deviations are ±0.05 and ±0.07C. These are of the same order of magnitude as the third effect, convergence on clean water, as calculated by Osborne (1965) and McGrath (1971). Clark (1967) gives a technique for distinguishing transmission effects from low lying mist or water vapor from genuine surface effects. With a single image at night, it is not always easy to distinguish air from water effects.

In summary, given an IR image of the ocean, the radiation surface temperature T_0 may fluctuate because T_w has changed, due perhaps to an isolated water mass, or to water from a vertical gradient stirred up from below. In the correction terms we may have changes in the boundary layer thickness induced by wind velocity, water velocity, air or sky temperature changes, boundary condition changes (contaminants), or changes in the emissivity or air transmission. We may have convergent flow, which accumulates contaminants, and has smaller effects on T_0 with clean water. In the following we give some examples of real images, with some tentative interpretation as to which of these mechanisms may be operating.

4. The partial interpretation of some infrared images

With the above background, let us examine Figs. 1–7 showing real bodies of water in nature. From Eq. (4) we see that certainly a major component of T_0 is T_w, the temperature of the underlying water. So, despite the complexities, hot water at the surface should show hot while cold water masses should show cold. Now we can certainly anticipate changes in T_w near the surface

from (i) intruding water masses as in the efflux from a power plant, or (ii) from stirring the water up from below, as in the wake of a ship or bridge pier. The second method is more complicated. If the water is isothermal, as it is to a considerable depth after several hours of night cooling, we may have to stir deeper (use a larger ship) at night than during the day. The stirring increases the turbulence (decreases the thickness of the water boundary layer) and may bring up contaminants (especially with air bubbles) to complicate the interpretation (Garrett, 1967). So let us take the simplest case first. Fig. 1 shows the discharge of a nuclear power plant by night and by day, and with opposite tidal currents. There are a number of points to be noted.

First, the boundary of hot and cold water is clearly defined. It is a commonplace observation in IR images that hot and cold water masses tend not to mix (i.e., they have a sharp boundary) *at a free surface,* but it is not at all obvious why this should be so. We suspect the reason is that the free surface tends to suppress all all three Cartesian components of turbulence (the vertical one obviously, due to buoyancy restraints). At some depth there may well be appreciable turbulent mixing of hot and cold water, but the infrared image shows only the surface itself, where the mixing is small.

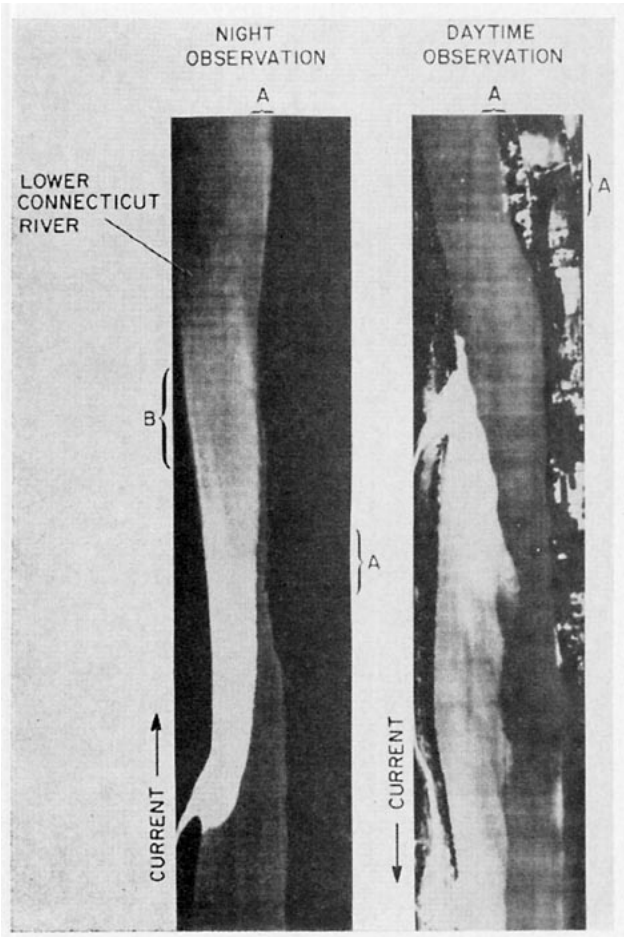

FIG. 1. Effluent from nuclear power plant at Haddam, Conn. (courtesy of Dr. R. W. Stingelin, HRB-Singer, Inc.).

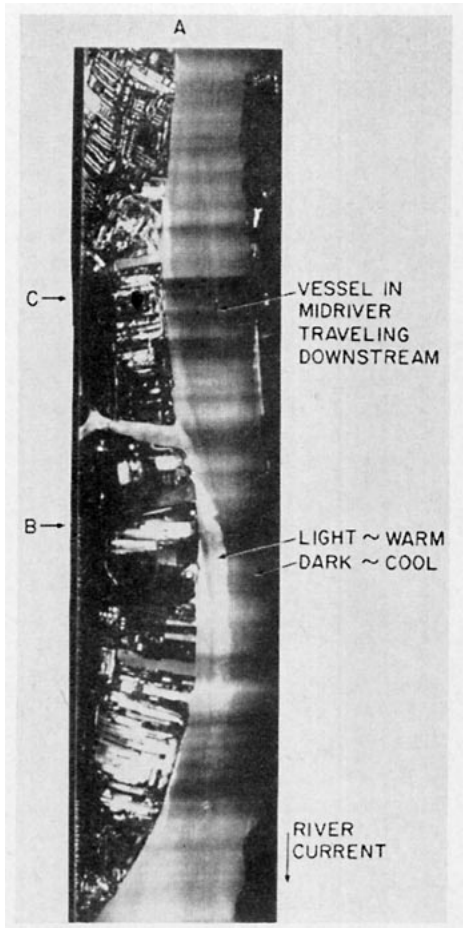

FIG. 2. Detroit River at night (courtesy of C. A. Bay, Raytheon Company).

Second, the thermal contrast in land detail at night is absent by comparison to daytime observations. From this we infer that several hours of nighttime cooling are probably sufficient to create an essentially isothermal surface. This nocturnal loss of detail could also be caused by a change of contrast setting of the equipment. Note that at A, some boat slips and a yacht basin or pier, which were relatively hot during the day, have cooled to slightly less than the water temperature at night. At B we note a slight separation of the hot water from the shoreline, which we suspect as being due to shallow water.

The above and what follows are inferences from the picture. Unfortunately, we do not have complete ground truth for these pictures.

Also note that in the upper left picture, when the warm water fades out downstream, there is no afterimage, or residual of opposite sign. If there were, one might suspect some chemical (surface) contaminants in the discharge. There is in Fig. 2 just the suggestion of evidence that this might be occurring.

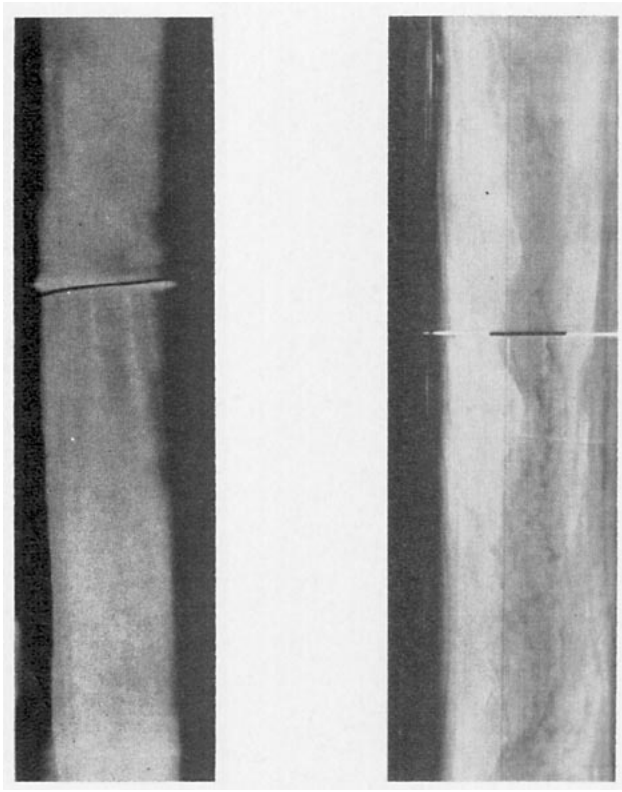

FIG. 3. Bridge piers' wakes in an estuary at night (courtesy of H. L. Clark, Naval Research Laboratory).

Fig. 2 shows the Detroit River at night, and in this case the land detail on the left bank, unlike in Fig. 1, is still showing very clearly. Some of these buildings are steel mills, and not likely to ever be cool. Several discharges of municipal waste water show on the left bank, but there is, in addition, beginning where discharge A fades out, a dark streak which can be traced down to where it merges with the outer edge of discharge B in the middle of the picture. This dark streak is most likely a surface contaminant. Whether it is a residual introduced at A, or a natural convergence or compaction due to the general river circulation, which piles up the natural contaminant on the river a short distance from the shoreline, we cannot say.

In the middle of the river at C is a white dot, presumably the stack of a tugboat pushing a line of barges (the short dark streak) downstream. Behind it, this configuration is leaving a faint light (warm) streak, which we identify as its wake.

Ship wakes at night are usually (not always) warm, as in this example. We interpret this to mean that stirring brings up isothermal water, so that this alone gives no signal. But the stirring alone does thin the water boundary layer which [as indicated by Eq. (2)] means a warm signal. We have seen examples where the warm wake fades out to be replaced by a cold one, which can be interpreted as a residual of contaminants (brought up by bubbles) making a thicker water boundary layer which appears cold. We have also seen examples where a ship wake crosses the sharp boundary of water mass of a given temperature to a water mass of different temperature. The wake temperature relative to the water mass in which it is stirred up changes sign at the water mass boundary. Wakes during the daytime or just after sunset in water which has a strong thermal gradient, can be cold (see Fig. 5). It is easy to calculate that the effects on T_0 of heating the water on engine discharge are negligible compared to the secondary effects just enumerated.

Fig. 3 shows examples of the turbulence behind bridge piers in a tideway at night (the Chesapeake Bay). Here the warm (whiter) wakes below the two piers supporting the main span over the channel are clearly discernible in both pictures. There are smaller wakes from neighboring piers. The sign is in agreement with the previous argument about turbulence in the isothermal nighttime water thinning the water boundary layer.

Close examination, particularly of the right-hand picture, will reveal some inexplicable anomalies. On that occasion there was a wind blowing at an angle to the tidal current. The initial direction of the dark streaks, emanating from the bridge at the same point as the hot (light) wakes, allowed the interpretation that these dark streaks were air wakes. Turbulence in the air thins the air boundary layer and gives an increased

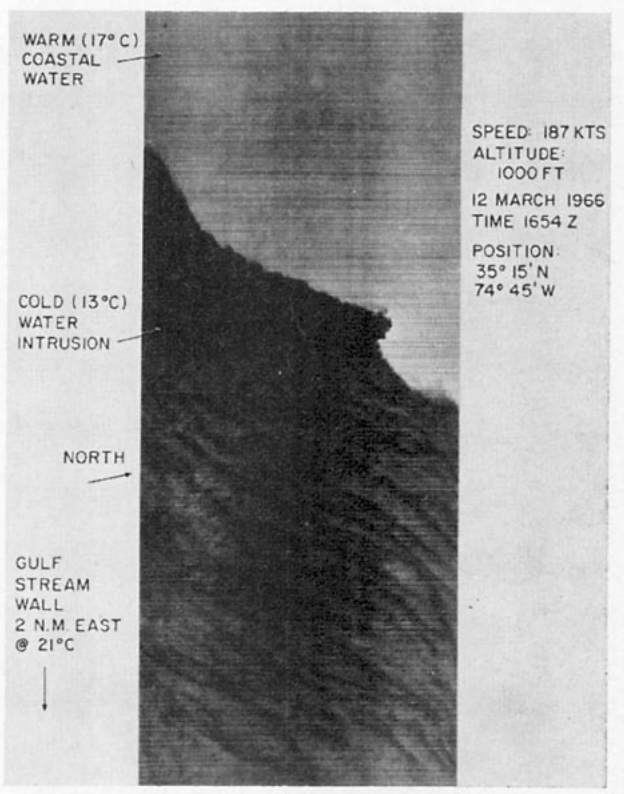

FIG. 4. Daytime imagery of an oceanic water mass boundary (courtesy of C. F. Beckner, Naval Oceanographic Office). Horizontal and vertical dimensions are 0.8 and 1.2 n mi, respectively.

evaporation rate and a cold signal in accordance with Eq. (2). So this explanation seems to fit, but there are difficulties and alternate possibilities. There is a sinuous dark pattern and the "wind wake" at least of the right-hand pier seems to follow this. The hot wakes from the pier seem not to participate in this sinuosity, but come off at right angles from the bridge. So one might ask, "Is the sinuosity and associated structure an air or water structure?" It could be that the previously identified air wakes are actually contaminants driven by the wind. Alternatively, the sinuosity might be a wind-driven pattern of water vapor, since the strict

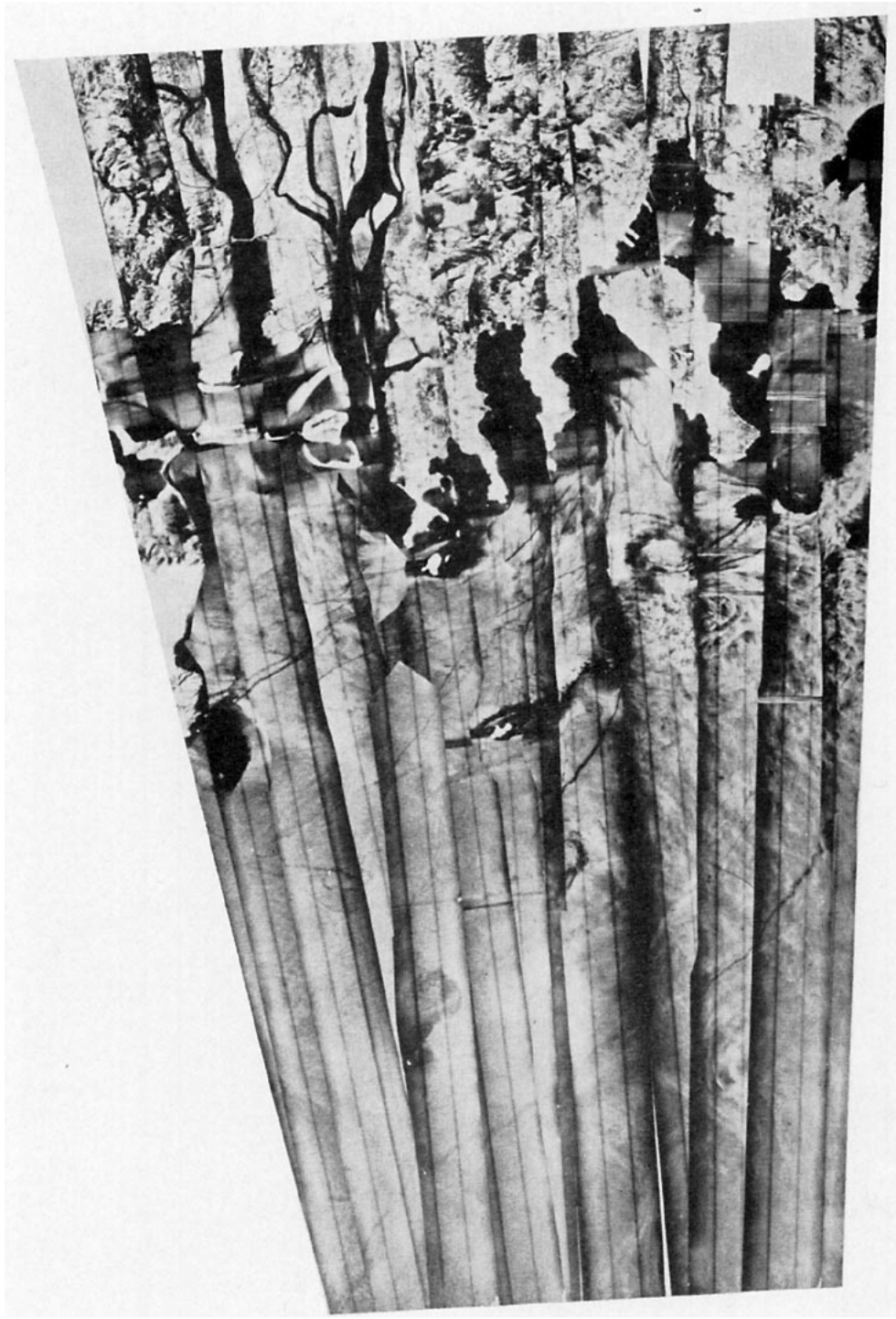

FIG. 5a. Ebb tide at Pusan Harbor, South Korea (courtesy of L. J. Fisher and D. R. Wisenet, Naval Oceanographic Office).

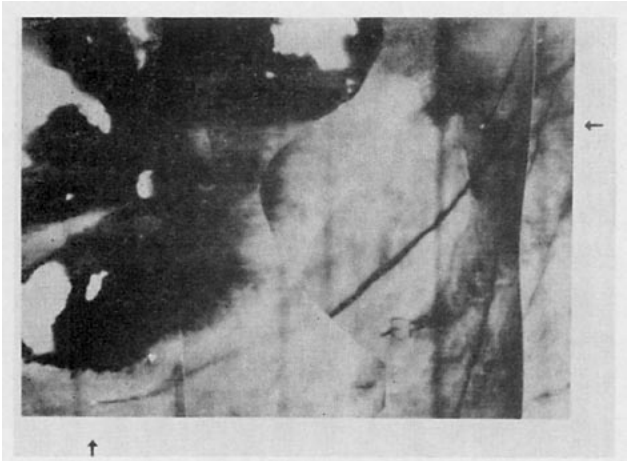

FIG. 5b. Enlargement of center. Arrows indicate boats generating wakes.

water wake of the piers seems not to follow it. We just don't know whether the sinuosity in the right-hand image of Fig. 3 is an air or water effect.

Fig. 4 shows a section of the boundary between two oceanic water masses of different surface temperatures. The temperatures were determined radiometrically by comparison to a source in the aircraft. There are two points to be noted: 1) the absence of detail in the warm mass (probably due to the limits of photographic reproduction, the full photographic range was set to correspond to less than 4C); and 2) the striations roughly parallel to the cool-warm water interface (a fairly common phenomenon). Close examination of the enlargements of Fig. 6 will show patches of similar structure. The striations of Fig. 4 are 50–100 m apart and are interpreted to indicate internal waves set up

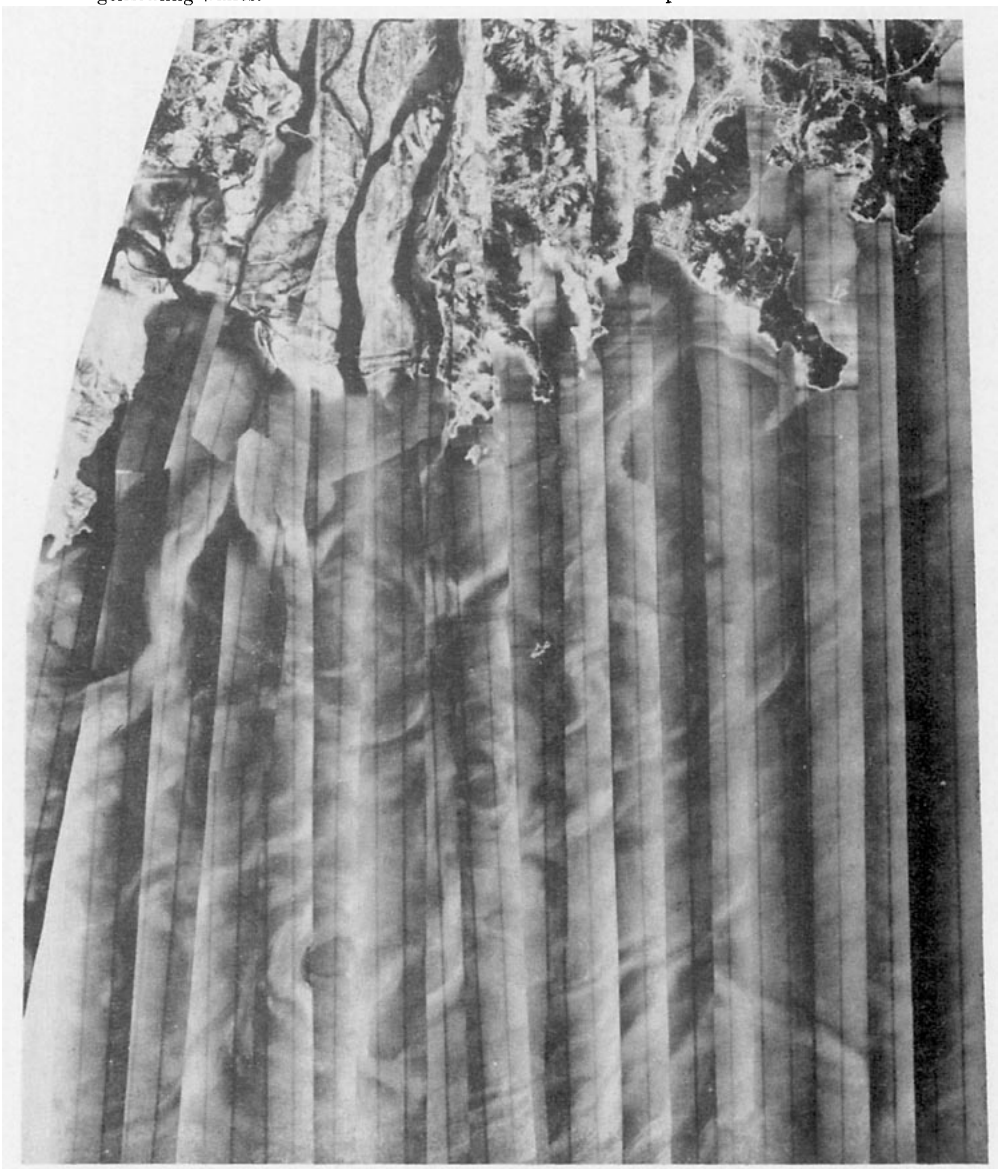

FIG. 6a. Flood tide at Pusan Harbor, South Korea (courtesy of L. J. Fisher and D. R. Wiesnet, Naval Oceanographic Office).

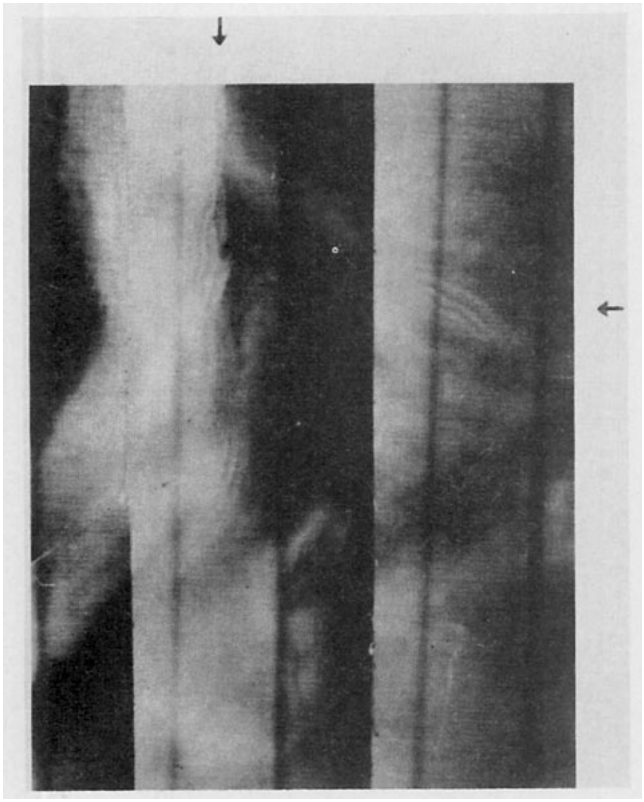

FIG. 6b. Enlargement of left center. Arrows indicate striations, similar to Fig. 4.

by the slow spreading of the hot water mass. Their thermal visibility is probably enhanced by the presence of a small amount of surface contaminant which is compacted or distended by the horizontal currents associated with the internal waves.

Figs. 5 and 6 are composite infrared images of Pusan Harbor, Korea, both taken in daylight on the same day, 5 hr apart on a flood and ebb tide. Note the contrast in the structure or "complexion" of the water surface in the two images. Fig. 5a (1115 local time) shows a fairly uniform surface temperature except for rather blotchy, closed-grained irregularities in the middle of the right-hand side of the picture. There are numerous narrow dark streaks which we interpret as boat wakes, cold water (plus contaminants) churned up from a greater depth (by contrast, at night wakes are more often hot). The enlargement (Fig. 5b) shows two of these wakes, terminated by a hot (white) dot, the generating boat.

Fig. 6a, in midafternoon (1630 local time) and the opposite tide, shows an irregular structure which covers the entire water surface. It has much larger average dimensions than the local blotchiness which appears in Fig. 5. Except in the lower left corner, there are no dark streaks or boat wakes whatsoever. We do not know whether this is due to a change in the water structure which renders wakes less visible, or whether there is simply less traffic at this time of day. The enlargement (Fig. 6b) shows some parallel striations

FIG. 7. Nighttime image off the Coast of Maine (courtesy of P. M. Moser, Naval Air Development Center).

similar to those we mentioned in connection with Fig. 4.

There are numerous details both in the land and water patterns in these pictures that we are totally unable to explain. We might mention that these two images of Pusan Harbor were made in an effort to find appropriate sites to place current and tide meters. Sites indicating any large vortex structure were to be avoided.

Finally, we show in Fig. 7 what resembles a "spiral nebula" observed from an aircraft at night over the Atlantic Ocean, about 100 mi off the coast of Maine. The white dots were reported as defects in the process of photographic development. It should not be assumed that the horizontal and vertical scales are exactly the same (Fig. 4). We do not know which way this object was spinning, whether it was expanding or contracting, or how long it lasted. It may be a water vapor structure. The linear dimensions are about 1 n mi.

5. Conclusion

It should be evident from the preceding discussion that interpreting IR ocean images is still in a primitive state. In the field one needs repeated observations of the same scene over current, wind and radiation changes, with simultaneous ground truth sufficient to disentangle the various phenomena which occur. In the laboratory, it remains to be shown that the various stability-instability transitions are as significant as we have surmised them to be, and that the postulated relation of drag and IR signal is valid. We emphasize the importance of varying the radiation or "sky" term. Theoretical developments are needed on the effects of contaminants on drag and boundary layer thickness. This problem is probably inseparable from the problem of wave generation, which has hitherto received the most theoretical attention.

Acknowledgments. The authors are grateful for the many helpful discussions with H. L. Clark and K. G. Williams of the Naval Research Laboratory which supported the work presented in this article. The authors are also indebted to the contributors and their organizations which are identified in the infrared photofacsimilies, Figs. 1–7.

APPENDIX

List of Symbols

δ_a	laminar air boundary layer thickness
δ_w	laminar water boundary layer thickness
σ	Stephan-Boltzmann constant
T_s	sky temperature
T_0	water surface radiation temperature
k_a	air molecular thermal conductivity
T_a	air temperature
k_w	water molecular thermal conductivity
T_w	bulk water temperature
ω_D	water vapor diffusivity coefficient
L	latent heat of vaporization
ρ_{amb}	ambient water vapor density in air
ρ_{sat}	saturated water vapor density in air
τ_a	cooling time constant in air $[=\delta_a^2/\kappa_w]$
τ_w	cooling time constant in water $[=\delta_w^2/\kappa_w]$
ΔT_c	temperature drop due to air and water conduction $[=(T_a-T_w)(k_a\delta_w/k_w\delta_a)]$
ΔT_r	temperature drop due to radiation $[=(T_s-T_w)(4\sigma T_w^3\delta_w/k_w)]$
ΔT_e	temperature drop due to evaporation $[=\omega_D L\delta_w(\rho_{\text{amb}}-\rho_{\text{sat}})/k_w\delta_a]$
κ_a	thermal diffusion coefficient in air
κ_w	thermal diffusion coefficient in water
U_{10}	wind speed at 10 m above mean water surface

REFERENCES

Ballard, S. S., 1959: A collection of papers on infrared measurements. *Proc. Inst. Rad. Eng.*, **47**, 1417–1419.

Batchelor, G. K., 1967: *Introduction to Fluid Dynamics*. Cambridge University Press, pp. 70, 147.

Boudreau, R. D., 1965: Skin temperature of the sea as determined by radiometer. Texas A & M Univ. Proj. Rept. 286. Available DDC.

Clark, H. L., 1967: Some problems associated with airborne radiometry of the sea. *Appl. Opt.*, **6**, 2151–2157.

Dobson, F. W., 1971: Pressure measurements on wind-generated sea waves. *J. Fluid Mech.*, **48**, 91–127.

Garrett, W. D., 1967: Damping of capillary waves at the air-sea interface by surface active material. *J. Marine Res.*, **15**, 279–291.

Goodrich, F. C., 1962: On the damping of water waves by monomolecular films. *J. Phys. Chem.*, **66**, 101–104.

Hasse, L., 1971: The sea surface temperature deviation and the heat flow at the air-sea interface. *Boundary-Layer Meteor.*, **1**, 368–379.

Hill, R. H., 1972: Laboratory measurement of heat transfer and thermal structure near an air-water interface. *J. Phys. Oceanogr.*, **2**, 190–198.

Kelton, Gilbert, *et al.*, 1963: Infrared target and background radiometric measurements, concepts, units and techniques. *Infrared Phys.*, **3**, 139–169.

Landau, L. D., and E. M. Lifschitz, 1959: *Fluid Mechanics*. London, Pergamon Press, pp. 214 and 217.

Lock, R. C., 1951: The velocity distribution in the laminar boundary layer between parallel streams. *Quart. J. Mech. Appl. Math.*, **4**, p. 42.

McDowell, R. S., and C. D. McCutcheon, 1971: The Thoreau-Reynolds ridge, a lost and found phenomena. *Science*, **172**, p. 973.

McGrath, J. R., 1971: An approximate linear theory treating heat and mass transfer through the laminar boundary layers at a sea surface disturbed by wave motion. Ph.D. dissertation, The Catholic University of America, Washington, D. C.

Osborne, M. F. M., 1964: The interpretation of infrared radiation from the sea in terms of its boundary layer. *Deut. Hydrogr. Z.*, **17**, 115–136.

——, 1965: The effect of convergent and divergent flow patterns on infrared and optical radiation from the sea. *Deut. Hydrogr. Z.*, **18**, 1–25.

——, 1968: The theory of the measurement of surface viscosity. *Kolloid Z. Polym.*, **224**, 150–161.

Phillips, O. M., 1966: *The Dynamics of the Upper Ocean.* Cambridge University Press, p. 144.

Roll, H. U., 1965: *Physics of the Marine Atmosphere.* New York, Academic Press, 161–163.

Ruggles, K. W., 1970: The vertical mean wind profile over the ocean for light to moderate winds. *J. Appl. Meteor.*, **9**, 389–395.

Schmitz, H. P., 1962: A relation between the vectors of stress, wind and current at water surfaces and between the shearing stresses and velocities at solid boundaries. *Deut. Hydrogr. Z.*, **15**, 23–36.

Stingelin, R. W., 1969: Operational airborne thermal imaging survey. *Geophysics*, **34**, 760–771.

Wu, J., 1971a: A note on sea spray and wind stress discontinuity. *Deep-Sea Res.*, **18**, 1041–1045.

——, 1971b: An estimation of oceanic thermal sublayer thickness. *J. Phys. Oceanogr.*, **1**, 284–286.